



Decoherence of Impurities in a Fermi Sea of Ultracold Atoms

Marko Cetina,^{1,2} Michael Jag,^{1,2} Rianne S. Lous,^{1,2} Jook T.M. Walraven,^{1,3} Rudolf Grimm,^{1,2}
Rasmus S. Christensen,⁴ and Georg M. Bruun⁴

¹*Institut für Quantenoptik und Quanteninformation (IQOQI), Österreichische Akademie der Wissenschaften,
6020 Innsbruck, Austria*

²*Institut für Experimentalphysik, Universität Innsbruck, 6020 Innsbruck, Austria*

³*Van der Waals-Zeeman Institute, Institute of Physics, University of Amsterdam,
Science Park 904, 1098 XH Amsterdam, Netherlands*

⁴*Department of Physics and Astronomy, Aarhus University, DK-8000 Aarhus C, Denmark*

(Received 10 June 2015; published 22 September 2015)

We investigate the decoherence of ^{40}K impurities interacting with a three-dimensional Fermi sea of ^6Li across an interspecies Feshbach resonance. The decoherence is measured as a function of the interaction strength and temperature using a spin-echo atom interferometry method. For weak to moderate interaction strengths, we interpret our measurements in terms of scattering of K quasiparticles by the Fermi sea and find very good agreement with a Fermi liquid calculation. For strong interactions, we observe significant enhancement of the decoherence rate, which is largely independent of temperature, pointing to behavior that is beyond the scattering of quasiparticles in the Fermi liquid picture.

DOI: [10.1103/PhysRevLett.115.135302](https://doi.org/10.1103/PhysRevLett.115.135302)

PACS numbers: 67.85.Lm, 03.75.Dg, 34.50.Cx, 71.38.-k

Many-body fermionic systems with strong interactions play a central role in condensed-matter, nuclear, and high-energy physics. The intricate quantum correlations between fermions challenge our understanding of these systems. Mixtures of ultracold fermionic gases offer outstanding opportunities to study strongly interacting fermions experimentally. Since the turn of the century, the excellent control over the strength of the interaction and the composition of these mixtures has allowed investigations addressing the broad spectrum from few-body to many-body phenomena [1,2]. Tuning of the interaction is achieved using Feshbach resonances [3]. The composition is varied by selecting internal states or by mixing different atomic species. This development has led to many exciting results concerning the quantum phases of fermionic mixtures, their excitations, superfluid behavior, and the equation of state [4].

In two-component fermionic systems with a large population imbalance, the minority atoms have been shown to form quasiparticles termed Fermi polarons, even for surprisingly large coupling strengths [5–8]. These are long-lived states described by Fermi liquid theory [9]. Their lifetime is limited by scattering against the majority atoms, which is suppressed by Pauli blocking as the temperature approaches zero [10,11]. Although the quasiparticle scattering rate has been determined in two-dimensional electron gases [12–14], measurements in well-defined three-dimensional (3D) fermionic systems have remained an experimental challenge.

Intriguing questions are related to the behavior of impurities and, more generally, Fermi mixtures in the strongly interacting regime [8,15,16]. For investigating an impurity in a Fermi sea, Refs. [17,18] suggested a

time-domain method that is applicable for a wide range of interaction strengths. This approach can be regarded as a measurement of the coherence of a superposition of internal states of the impurity atoms using interferometry [19]. Atom coherence has previously been used to probe many-body demagnetization in fermionic systems [20] and impurity scattering in bosonic systems [21].

In this Letter, we report on measurements of decoherence of K atoms immersed in a Fermi sea of Li using the method proposed in Ref. [18] in the regime of strong population imbalance. We tune the interaction between the Li and K atoms using an interspecies Feshbach resonance (FR). For weak to moderately strong interactions, we interpret the measured decoherence in terms of the scattering of K quasiparticles by the Li Fermi sea. We find very good agreement with a Fermi liquid calculation. This provides a determination of the quasiparticle scattering rate in a clean 3D fermionic system. We extend our measurements to strong Li-K interactions and find decoherence rates that are comparable to the fastest dynamics available in our system. These rates do not increase with temperature, which is an indication of zero-temperature quantum dynamics in a fermionic many-body system.

The starting point of our experiments is an evaporatively cooled, thermally equilibrated mixture of, typically, 3×10^5 ^6Li atoms and 1.5×10^4 ^{40}K atoms, trapped in a crossed-beam 1064-nm optical dipole trap under conditions similar to those in Ref. [6]. The Li cloud is degenerate, with $k_B T / \epsilon_F$ as low as 0.15, where T is the temperature and $\epsilon_F \approx h \times 35$ kHz is the average Li Fermi energy sampled by the K atoms. Because of the Li Fermi pressure and the more than two times stronger optical potential for K, the K cloud is

much smaller than the Li cloud [22] and, therefore, samples a nearly homogenous Li environment, with a standard deviation in the local Li Fermi energy of less than $0.1\epsilon_F$. In spite of the smaller size of the K cloud, the concentration of K in the Li sea remains low, with $\bar{n}_K/\bar{n}_{Li} \approx 0.3$, where \bar{n}_K (\bar{n}_{Li}) is the average K (Li) number density sampled by the K atoms. The K ensemble is correspondingly nondegenerate, with $k_B T/E_F^K > 0.9$, where E_F^K is the peak K Fermi energy.

We tune the interaction between the K and Li atoms using an interspecies FR between the Li atoms in the lowest Zeeman sublevel Li|1) and K atoms in the third-lowest sublevel K|3) [23]. We quantify the interactions between Li and K by the dimensionless interaction parameter $-1/\kappa_F a$, where $\kappa_F = \hbar^{-1}\sqrt{2m_{Li}\epsilon_F}$ is the Li Fermi wave number with m_{Li} the Li mass, and a is the s -wave interspecies scattering length. The latter can be tuned as $a = a_{bg}[1 - \Delta/(B - B_0)]$ by applying a magnetic field B , where $B_0 \approx 154.7$ G is the resonance center, $a_{bg} = 63.0 a_0$ (a_0 is Bohr's radius) and $\Delta = 880$ mG [23]. The relatively narrow nature of our FR causes significant momentum dependence of the interspecies interaction. We characterize this effect by the length parameter R^* [6,24]. In our experiments, $\kappa_F R^*$ is approximately 0.9, corresponding to an intermediate regime where the interaction is near universal with substantial effective-range effects.

We probe the decoherence of the K atoms using a radio-frequency (rf) interferometric technique, as illustrated in Fig. 1. The K atoms are initially prepared in the

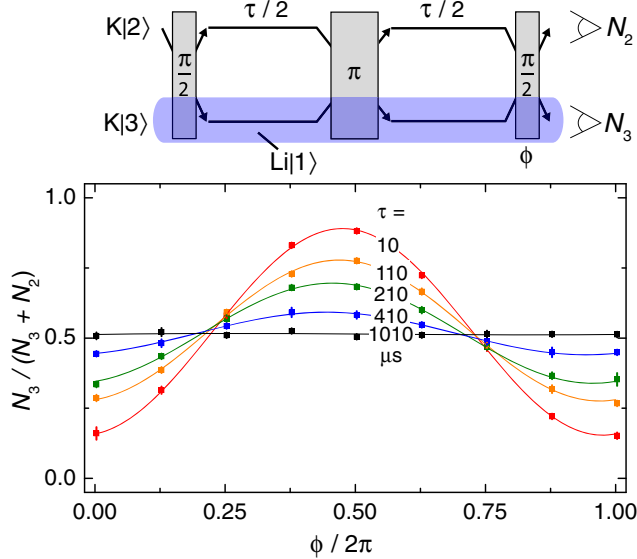


FIG. 1 (color online). Interferometric method for measuring the decoherence of K in a Li Fermi sea. The upper illustration shows a schematic of the rf pulse sequence. The atoms in the K|3) state interact with a Fermi sea of Li|1) atoms, as indicated by the shaded region. The graph shows the fraction of the K atoms transferred to the K|3) state as a function of the relative phase of the final $\pi/2$ rf pulse for various interaction times τ and for $-1/\kappa_F a = 2.1$, $T = 0.16 \epsilon_F/k_B$.

second-lowest Zeeman sublevel K|2) while the Li atoms remain in the Li|1) state throughout the experiment. On the time scale of our measurements, the interactions between these atoms, characterized by the s -wave scattering length $a_{12} \approx a_{bg}$, can be neglected. We apply a $\pi/2$ rf pulse (typically 10 μ s long) to prepare the K atoms in an equal superposition of the K|3) and K|2) states. After a variable interaction time τ , we apply a second $\pi/2$ rf pulse before determining the numbers N_2 and N_3 of atoms in the K|2) and K|3) states using absorption imaging [25]. To decrease the sensitivity to the magnetic field noise and to the inhomogeneities in the atom densities, we perform a spin echo by splitting the interaction time into two equal halves separated by a π rf pulse.

Shifting the phase of the rf oscillator by ϕ between the π and the second $\pi/2$ pulses causes a sinusoidal variation in the fraction $f = N_3/(N_2 + N_3)$ of the K atoms transferred to K|3), as shown in Fig. 1. We quantify the coherence of the state of the K atoms by the contrast $C = (f_{\max} - f_{\min})/(f_{\max} + f_{\min})$ of these oscillations. The interaction of the K atoms with the Li cloud causes an exponential decrease in the observed contrast with increasing interaction time τ , as shown in Fig. 2(a). The interaction also shifts the rf transition frequency and decreases the rf coupling between the K|2) and K|3) states [6], which we account for by adjusting the rf frequency and the duration of our rf pulses. In this way, we measure the decoherence of K atoms for $-1/\kappa_F a < -0.8$ and $-1/\kappa_F a > 1.4$. Near the center of the resonance, the fast

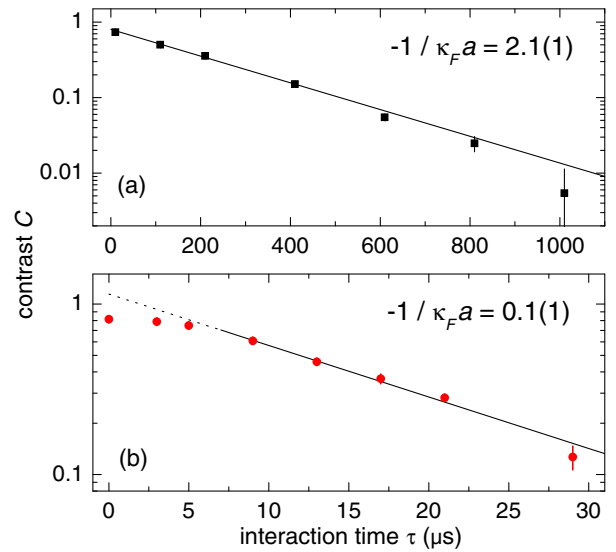


FIG. 2 (color online). Contrast C as a function of interaction time τ . In (a), we show results for moderately attractive interspecies interactions ($-1/\kappa_F a = 2.1$), corresponding to Fig. 1. In (b), we probe the system in the strongly interacting regime ($-1/\kappa_F a = 0.15$) for $T = 0.20 \epsilon_F/k_B$ by rapidly shifting the interaction parameter from 2.2 to 0.15 during the interaction time. The solid lines are exponential fits to the points with $\tau > 7 \mu$ s. The dotted line is an extrapolation to $\tau = 0$.

loss of contrast during the rf pulses limits the applicability of this method.

To measure the decoherence of K in the strongly interacting regime, we use laser light to rapidly displace our magnetic FR [32–34]. Optical control of our FR allows us to apply the rf pulses away from the FR and then rapidly bring the atoms into resonance for the duration of the interaction time τ [35]. This method circumvents the loss of contrast during the rf pulses and allows us to probe the K decoherence across the full range of interaction parameters. The displacement of our FR arises from the laser-induced differential ac Stark shift between the free-atom level and the molecular state involved in the FR. The ac Stark shift is induced by the 1064-nm trapping light, as we investigated in Ref. [36]. Although the differential shift here amounts to only 10% of the total trapping potential, using a high-intensity beam with up to 65 kW/cm², we can displace B_0 by up to 40 mG in less than 200 ns—all while preserving the harmonic trapping potential [25]. This displacement corresponds to a change in the interaction parameter of up to ± 2.1 on a time scale of $0.05 \tau_F$, where $\tau_F = \hbar/\epsilon_F \approx 4.5 \mu\text{s}$ is the Fermi time.

In Fig. 2(b), we show the dependence of the contrast C on the interaction time τ near the center of our FR. The contrast starts to decay after an initial delay of approximately τ_F . This delay can be explained in terms of quantum evolution of the system with an interaction energy bounded from above by ϵ_F [18]. For $\tau > 1.6 \times \tau_F \approx 7 \mu\text{s}$, the decrease in contrast is well described by an exponential decay. The fitted rate $\gamma_{\text{coh}} = 0.28(2) \tau_F^{-1}$ is comparable to the inverse Fermi time, indicating that our experiment cannot be fully described by the scattering of quasiparticles in the Fermi liquid picture, which assumes long-lived quasiparticles [9].

In Fig. 3, we show the dependence of the fitted rate γ_{coh} on the interaction parameter. We present data with two decades of dynamic range and demonstrate a dramatic resonant enhancement of the decoherence rate, reaching values up to $0.4 \tau_F^{-1}$. The data do not exhibit any clear dependence on $\bar{n}_K/\bar{n}_{\text{Li}}$ across the full range $0.17 \leq \bar{n}_K/\bar{n}_{\text{Li}} \leq 0.43$. In addition to the statistical errors indicated by the error bars, the data are subject to variations of $k_B T/\epsilon_F$, $\kappa_F R^*$, and $\bar{n}_K/\bar{n}_{\text{Li}}$ with standard deviations of 0.01, 0.02, and 0.07 about their mean values of 0.16, 0.93, and 0.27, respectively. The calibration of the Li atom number introduces a 6% systematic uncertainty in ϵ_F and τ_F , as well as a corresponding 3% uncertainty in κ_F . Further, our total error budget includes 3% systematic errors in a and R^* arising from the uncertainty in ΔB and a ± 0.05 error in $1/\kappa_F a$ resulting from an uncertainty in the determination of B_0 of ± 1 mG [25].

For weak to moderate interactions, there are well-defined K quasiparticles, and we now show that the evolution of the contrast C on time scales much longer than τ_F can be related to the mean quasiparticle scattering rate γ_s . Each

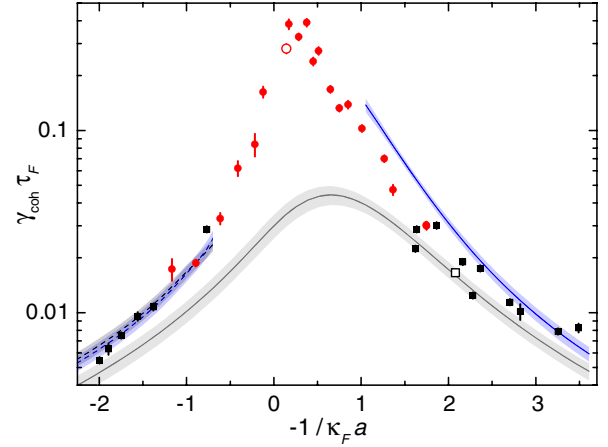


FIG. 3 (color online). Decoherence rate of K in a Li Fermi sea as a function of the interaction parameter for an average temperature $T = 0.16 \epsilon_F/k_B$ (see text). The measurements with (with-out) rapid shifting of the FR are shown as the red circles (black squares). The measurements from Fig. 2 are indicated by open symbols. The solid upper (blue) and lower (black) lines correspond to the prediction of the Fermi liquid theory with and without medium corrections, respectively. The dashed lines incorporate corrections due to decay to Feshbach molecules. The shaded areas show the 1σ effect of the experimental uncertainties on the theoretical predictions.

scattering event provides which-way information that distinguishes between the two paths in the interferometer in Fig. 1 and, thus, erases the interference effect. At any given time, the interaction affects only one of the two paths, decreasing the probability for the system to stay in this path at the rate γ_s . Since our signal arises from the interference of the amplitudes in the two interferometer paths, we expect the interaction to lead to a decrease of the observed contrast at the rate $\gamma_s/2$.

From Fermi liquid theory, the scattering rate γ_{p_1} of a K quasiparticle with momentum \mathbf{p}_1 is given by [9]

$$\gamma_{p_1} = \iint d\check{p}_2 d\Omega \frac{m_r p_r}{4\pi^2} |\mathcal{T}|^2 [f_{p_2}^{\text{Li}}(1 - f_{p_3}^{\text{K}} - f_{p_4}^{\text{Li}}) + f_{p_3}^{\text{K}} f_{p_4}^{\text{Li}}]. \quad (1)$$

Here, \mathcal{T} is the scattering matrix for the scattering of K atoms with Li atoms with momenta \mathbf{p}_1 and \mathbf{p}_2 , respectively, to momenta \mathbf{p}_3 and \mathbf{p}_4 . We have defined $d\check{p}_2 = d^3 p_2 / (2\pi)^3$, and Ω is the solid angle for the direction of the outgoing relative momentum. The distribution functions are $f_p^{\text{Li/K}} = [e^{\beta(E_p^{\text{Li/K}} - \mu_{\text{Li/K}})} + 1]^{-1}$ with the chemical potentials $\mu_{\text{Li/K}}$ for the Li/K atoms, respectively. The dominant medium effects can be shown to enter in the scattering matrix \mathcal{T} via ladder diagrams, whereas the quasiparticles can be assumed to have the ideal gas energy dispersion $E_p^{\text{K/Li}} = p^2/2m_{\text{K/Li}}$ [37,38]. The details of the calculation of γ_{p_1} are described in [39]. In addition, we

account for the reduced quasiparticles' residue Z by multiplying the collision rate by Z calculated from the ladder approximation [8]. To obtain the mean scattering rate γ_s , we calculate the thermal average $\gamma_s = \int d\vec{p} f_p^K \gamma_p$. To include the effects of the trap, we use effective Fermi energies, which are obtained by averaging the local Fermi energy over the density of the K atoms in the trap. This approach is justified since the K atoms only probe a small region of the Li gas, and because the momentum distribution of the K atoms is nearly classical.

On the repulsive side of the FR, we need to consider additional effects arising from the decay of the atoms into the molecular state that underlies our FR. The rate Γ of this process was calculated and confirmed by measurements in Ref. [6], reaching values as high as $0.02 \tau_F^{-1}$ close to resonance. Since the decay to molecules provides which-way information, it will contribute at least $\Gamma/2$ to the measured decoherence rate. The decay also releases energy and creates holes in the Li Fermi sea, increasing the value of $k_B T / \epsilon_F$ during our measurement to $0.20(1)$ [25].

In Fig. 3, we plot the calculated decoherence rate $\gamma_s/2$ as a function of the interaction parameter. The lower solid line is obtained by using the vacuum scattering matrix \mathcal{T}_{vac} [39] in (1), whereas the upper solid line is obtained by using a \mathcal{T} matrix which includes medium effects using the ladder approximation. The dashed lines include the effects of decay into the molecular state. The calculated decoherence rate agrees with the experimental values very well for $-1/k_F a \gtrsim 1.5$ and for $-1/k_F a \lesssim -1$. This gives strong evidence that the observed decoherence is, indeed, due to quasiparticle collisions. The significant asymmetry of the decoherence rate around $1/k_F a = 0$ arises from the narrow nature of the FR [39]. The calculated decoherence rate is larger when medium effects are included in the \mathcal{T} matrix. This is due to pair correlations, which can increase the collisional cross section significantly [39]. We see that the inclusion of these medium effects on the scattering matrix improves the agreement with the experimental data. For stronger interactions, the calculation does not fit the experiment, which is expected since there are no well-defined quasiparticles in the unitarity regime [6]. Our model agrees with the observed absence of a dependence of γ_{coh} on $\bar{n}_K/\bar{n}_{\text{Li}}$ since the K cloud is close to the classical regime where $f_{p_3}^K \ll 1$ and the momentum distribution of the K atoms is solely determined by the temperature.

Further insight into the nature of the observed decoherence can be gained by varying the temperature of our atom mixture, which we accomplish by changing the endpoint of our evaporative cooling. We show the dependence of the measured decoherence rate on temperature in Fig. 4. In addition to the statistical errors shown by the error bars, the data are subject to small variations of $-1/k_F a$, $\kappa_F R^*$, and $\bar{n}_K/\bar{n}_{\text{Li}}$ with standard deviations of 0.05, 0.03, and 0.1, respectively. Our total error budget also includes

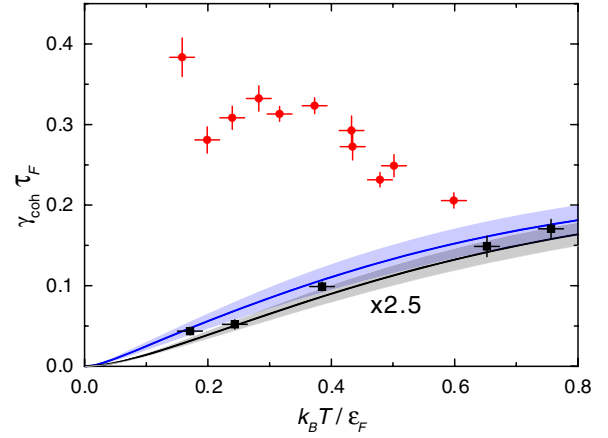


FIG. 4 (color online). Decoherence rate of K in a fermionic Li cloud as a function of temperature. The data for $-1/\kappa_F a = 0.2$, $\kappa_F R^* = 0.94$, $\bar{n}_K/\bar{n}_{\text{Li}} = 0.2$ ($-1/\kappa_F a = 2.4$, $\kappa_F R^* = 0.89$, $\bar{n}_K/\bar{n}_{\text{Li}} = 0.3$) measured with (without) rapid shifting of the FR is shown as red circles (black squares). The solid blue and black lines correspond to the predictions of the Fermi liquid theory for $-1/\kappa_F a = 2.4$ with and without medium corrections, respectively. The shaded areas show the 1σ effect of the experimental uncertainties on the theoretical predictions.

the above-mentioned systematic uncertainties in ϵ_F , κ_F , a , and R^* .

Away from the FR, the measured decoherence rates are in very good agreement with the predictions of the Fermi liquid theory. The linear dependence of γ_{coh} on temperature in this regime arises from the high relative mass of the K atoms, causing the Li-K scattering to resemble scattering by fixed impurities. This is similar to the situation in metals where the scattering of electrons by fixed nuclei gives rise to the well-known linear dependence of the nuclear decoherence rates on temperature [40]. The red circles in Fig. 4 represent the measurements for resonant interactions. The rates obtained in this regime are more than an order of magnitude higher than the off-resonant rates and do not increase with temperature.

In conclusion, we established that, for weak to moderate interaction strengths, the decoherence of K in a Li Fermi sea is dominated by quasiparticle scattering. Our observations for strong interactions cannot be explained solely by quasiparticle scattering and indicate decoherence processes which persist at zero temperature. This offers an exciting opportunity to explore the many-body quantum dynamics of an impurity submerged in a Fermi sea.

We thank F. Schreck, C. Kohstall, I. Fritsche, P. Jeglič, Y. Ohashi, R. Schmidt, E. Demler, and, especially, M. Parish, J. Levinsen, and M. Baranov for helpful discussions. We thank P. Massignan for sending us data for the quasiparticle residue and decay. We acknowledge funding by the Austrian Science Fund FWF within the Special Research Program FoQuS (Project No. F40-P04) and support of the Villum Foundation via Grant No. VKR023163.

- [1] I. Bloch, J. Dalibard, and W. Zwerger, *Rev. Mod. Phys.* **80**, 885 (2008).
- [2] S. Giorgini, L. P. Pitaevskii, and S. Stringari, *Rev. Mod. Phys.* **80**, 1215 (2008).
- [3] C. Chin, R. Grimm, P. S. Julienne, and E. Tiesinga, *Rev. Mod. Phys.* **82**, 1225 (2010).
- [4] M. W. Zwierlein, in *Novel Superfluids*, edited by K.-H. Bennemann and J. B. Ketterson (Oxford University Press, Oxford, 2015), Vol. 2, Chap. 18.
- [5] A. Schirotzek, C.-H. Wu, A. Sommer, and M. W. Zwierlein, *Phys. Rev. Lett.* **102**, 230402 (2009).
- [6] C. Kohstall, M. Zaccanti, M. Jag, A. Trenkwalder, P. Massignan, G. M. Bruun, F. Schreck, and R. Grimm, *Nature (London)* **485**, 615 (2012).
- [7] M. Koschorreck, D. Pertot, E. Vogt, B. Frölich, M. Feld, and M. Köhl, *Nature (London)* **485**, 619 (2012).
- [8] P. Massignan, M. Zaccanti, and G. M. Bruun, *Rep. Prog. Phys.* **77**, 034401 (2014).
- [9] G. Baym and C. Pethick, *Landau Fermi Liquid Theory* (Wiley-VCH, Weinheim, 1991).
- [10] L. Landau, *Sov. Phys. JETP* **5**, 101 (1957).
- [11] L. Landau, *Sov. Phys. JETP* **3**, 920 (1957).
- [12] Y. Berk, A. Kamenev, A. Palevski, L. N. Pfeiffer, and K. W. West, *Phys. Rev. B* **51**, 2604 (1995).
- [13] S. Q. Murphy, J. P. Eisenstein, L. N. Pfeiffer, and K. W. West, *Phys. Rev. B* **52**, 14825 (1995).
- [14] M. Slutzky, O. Entin-Wohlman, Y. Berk, A. Palevski, and H. Shtrikman, *Phys. Rev. B* **53**, 4065 (1996).
- [15] S. Nascimbène, N. Navon, S. Pilati, F. Chevy, S. Giorgini, A. Georges, and C. Salomon, *Phys. Rev. Lett.* **106**, 215303 (2011).
- [16] Y. Sagi, T. E. Drake, R. Paudel, R. Chapurin, and D. S. Jin, *Phys. Rev. Lett.* **114**, 075301 (2015).
- [17] J. Goold, T. Fogarty, N. Lo Gullo, M. Paternostro, and T. Busch, *Phys. Rev. A* **84**, 063632 (2011).
- [18] M. Knap, A. Shashi, Y. Nishida, A. Imambekov, D. A. Abanin, and E. Demler, *Phys. Rev. X* **2**, 041020 (2012).
- [19] A. D. Cronin, J. Schmiedmayer, and D. E. Pritchard, *Rev. Mod. Phys.* **81**, 1051 (2009).
- [20] A. B. Bardon, S. Beattie, C. Luciuk, W. Cairncross, D. Fine, N. S. Cheng, G. J. A. Edge, E. Taylor, S. Zhang, S. Trotzky *et al.*, *Science* **344**, 722 (2014).
- [21] R. Scelle, T. Rentrop, A. Trautmann, T. Schuster, and M. K. Oberthaler, *Phys. Rev. Lett.* **111**, 070401 (2013).
- [22] A. Trenkwalder, C. Kohstall, M. Zaccanti, D. Naik, A. I. Sidorov, F. Schreck, and R. Grimm, *Phys. Rev. Lett.* **106**, 115304 (2011).
- [23] D. Naik, A. Trenkwalder, C. Kohstall, F. M. Spiegelhalter, M. Zaccanti, G. Hendl, F. Schreck, R. Grimm, T. Hanna, and P. Julienne, *Eur. Phys. J. D* **65**, 55 (2011).
- [24] D. S. Petrov, *Phys. Rev. Lett.* **93**, 143201 (2004).
- [25] See Supplemental Material at <http://link.aps.org/supplemental/10.1103/PhysRevLett.115.135302> for details on determination of the absolute atom numbers, the state-sensitive atom detection, the optical shifting of the FR, the resonance position determination, and the estimate of the heating due to decay to Feshbach molecules, which includes Refs. [26–31].
- [26] A. B. Ruffin, in *NIST Symposium on Optical Fiber Measurements*, Technical Digest (National Institute of Standards and Technology, Boulder, Colorado, 2004), pp. 23–28.
- [27] A. D. Lange, K. Pilch, A. Prantner, F. Ferlaino, B. Engeser, H.-C. Nägerl, R. Grimm, and C. Chin, *Phys. Rev. A* **79**, 013622 (2009).
- [28] C. Chin and P. S. Julienne, *Phys. Rev. A* **71**, 012713 (2005).
- [29] W. I. McAlexander, E. R. I. Abraham, and R. G. Hulet, *Phys. Rev. A* **54**, R5 (1996).
- [30] P. Massignan, *Europhys. Lett.* **98**, 10012 (2012).
- [31] K. Huang, *Statistical Mechanics* (John Wiley & Sons, Inc., Hoboken, USA, 1987).
- [32] D. M. Bauer, M. Lettner, C. Vo, G. Rempe, and S. Dürr, *Nat. Phys.* **5**, 339 (2009).
- [33] D. M. Bauer, M. Lettner, C. Vo, G. Rempe, and S. Dürr, *Phys. Rev. A* **79**, 062713 (2009).
- [34] L. W. Clark, L.-C. Ha, C.-Y. Xu, and C. Chin, [arXiv:1506.01766](https://arxiv.org/abs/1506.01766).
- [35] For measurements on the attractive (repulsive) side of the FR, we shift B_0 upwards (downwards). For measurements near the resonance, we verify that the direction of the shift of B_0 does not affect the result.
- [36] M. Jag, M. Zaccanti, M. Cetina, R. S. Lous, F. Schreck, R. Grimm, D. S. Petrov, and J. Levinsen, *Phys. Rev. Lett.* **112**, 075302 (2014).
- [37] G. M. Bruun and H. Smith, *Phys. Rev. A* **72**, 043605 (2005).
- [38] T. Enss, *Phys. Rev. A* **86**, 013616 (2012).
- [39] R. S. Christensen and G. M. Bruun, *Phys. Rev. A* **91**, 042702 (2015), for the relevant parameter r_{eff} , see [24].
- [40] J. Korrington, *Physica* **16**, 601 (1950).